

Evidence for Spring Loaded Inverted Pendulum Running in a Hexapod Robot

Richard Altendorfer, Uluç Saranlı, Haldun Komsuoğlu, Daniel Koditschek
Artificial Intelligence Laboratory, University of Michigan
Ann Arbor, MI 48109
{altendor, ulucs, hkomsuog, kod}@eecs.umich.edu

H. Benjamin Brown Jr.
The Robotics Institute, Carnegie Mellon University
Pittsburgh, PA 15213
hbb+@cs.cmu.edu

Martin Buehler, Ned Moore, Dave McMordie
Ambulatory Robotics Laboratory, Dept. of Mech. Engineering, McGill University
Montréal, Québec, Canada H2A 2A7
{buehler, ned, mcmordie}@cim.mcgill.ca

Robert Full
Dept. of Integrative Biology, University of California at Berkeley
Berkeley, CA 94720
rjfull@socrates.berkeley.edu

Abstract:

This paper presents the first evidence that the Spring Loaded Inverted Pendulum (SLIP) may be “anchored” in our recently designed compliant leg hexapod robot, RHex. Experimentally measured RHex center of mass trajectories are fit to the SLIP model and an analysis of the fitting error is performed. The fitting results are corroborated by numerical simulations. The “anchoring” of SLIP dynamics in RHex offers exciting possibilities for hierarchical control of hexapod robots.

1. Introduction

We have recently reported on a prototype robot that breaks new ground in artificial legged locomotion [1]. Our shoe-box sized, compliant leg hexapod, RHex, travels at speeds better than one body length per second over terrain that few other robots can negotiate at all. RHex origins and construction are grounded in the interplay between biomechanics, controls, and engineering design that we have come to call “functional biomimesis.” We aim to articulate broad principles with mathematically precise formulations of biomechanically observed fact and then translate these into specific design practices. This paper presents the first empirical evidence that our strategy to use a low degree

of freedom mechanism as a “template” for a high degree of freedom task may be relevant and productive. Biomechanics research suggests that the Spring Loaded Inverted Pendulum (SLIP) functions as a sagittal plane template for all animal running [2]. Motivated by the success of Raibert’s hoppers [3] that explicitly incorporate a physical SLIP in the working mechanism, we had previously begun to develop a theory to inform SLIP tuning [4]. We had also reported simulation evidence describing how the two degree of freedom SLIP template might be anchored in a four degree of freedom (all revolute) bipedal running model [5]. Adapting well-characterized methods developed at the UC Berkeley Polypedal lab to explore gait stabilization in animals and a model introduced in [1], we now offer a preliminary characterization of RHex center of mass (COM) trajectories respecting which the presumed relevance of the SLIP model can be empirically tested.

2. The SLIP Template for Legged Runners

A template [6] is a low dimensional model of a robot operating within a specified environment that is capable of expressing a specific task as the limit set of a suitably tuned dynamical system involving some controlled (robot) and uncontrolled (environment) degrees of freedom. To “anchor” this low dimensional model in a more physically realistic higher degree of freedom representation of the robot and its environment, we seek controllers whose closed loops result in a low dimensional attracting invariant submanifold on which the restriction dynamics is a copy of the template. Examples of this idea at work in functioning robots include a series of batting machines that anchored a “Raibert vertical” template [7] in a one degree of freedom paddle robot (operating into a two degree of freedom environment) [8] and a three degree of freedom paddle robot (operating into a three degree of freedom environment) [9]. This same idea is used to control a recently reported brachiating robot [10]. In this section we review the manner in which a hierarchical controller can be devised to shape and then exploit the appearance of the SLIP template in morphologically distinct legged machines.

2.1. Hierarchical Control of a Virtual SLIP Monopod

Biomechanical evidence for the existence of a SLIP template in human runners [11, 12] naturally leads to the possibility of template based controller designs for legged locomotion. Toward this end, previous work [5] demonstrated an approximate embedding of a SLIP template in a planar 4 DOF leg with ankle, knee and hip joints (AKH), similar in morphology to a human leg.

The hierarchical control of AKH involves defining a virtual leg between the toe and the COM of the system. The joint control torques are then computed using a SLIP template prescribing the ground reaction force (and hence the acceleration of the COM) together with an approximate, virtual work based embedding. In consequence of this hierarchical decomposition, a high level SLIP controller can be used to regulate the speed and hopping height of the overall system.

This approach to hierarchical design bears useful comparison to the notion

of impedance control advanced by Hogan [13] and more recently introduced into the locomotion literature in the more specific form of “Virtual Model Control” by Pratt and colleagues [14]. This framework allows a user to program the robot’s task in terms of a reference compliance imposed on a targeted part of the body. It is different from our approach in that the allowable reference models operate in the quasi-static regime, so, for example, running could not lie within the formal scope of the method. In contrast, the SLIP template provides an explicitly (hybrid) dynamical specification of the exchange between kinetic and potential energy that accomplishes the task at hand after transients in the many degrees of freedom unrelated to the task have died out. In this paper, we are concerned to find a means of effecting this “collapse of dimension” in the RHex mechanics.

2.2. Hierarchical Control of a Virtual SLIP Hexapod

We now describe two alternative approaches to hierarchical control for our hexapod. Both appeal to the SLIP template for the prescription of COM forces, but incorporate different anchoring mechanisms.

The hexapod model we consider is a rigid body with six massless legs [1]. Two of the spherical leg freedoms — the radial length and one of the angles — are driven by passive springs and dampers, whereas the hip angle is torque actuated. Consequently, there are only six actuated joints, and the overall system has six degrees of freedom, all due to the rigid body.

2.2.1. Active Control

In principle, the force and torque acting on the hexapod rigid body can be determined using the equations of motion of the model [1]. Sufficient conditions for exact embedding of an arbitrary dynamical template can be developed from the invertibility of the dynamics. However, complete input invertibility generally cannot prevail in our system. The morphology of the system, the hybrid nature of the problem and the structure and number of the actuators (especially when not all legs are on the ground) do not yield full control over the six body degrees of freedom.

A simpler planar model, on the other hand, provides an exactly invertible plant, except for co-dimension one and two singularities. The model consists of a three degree of freedom planar rigid body, with six torque actuated massless legs, with the assumption that three or more legs are in contact with the ground during stance.

Preliminary numerical experience with this model suggests that choosing a “reasonable” stance posture affords inverse dynamics controllers that pass transversally through the kinematic singularities and give good SLIP trajectories. Moreover, the planar model is structurally very close to the spatial model. As a consequence, it seems likely that the inverse dynamics anchoring in the planar model can be readily extended to yield an approximate embedding of the SLIP template in the spatial hexapod model.

Nevertheless, realizing the active template through inverse dynamics control suffers the traditional problems of all such approaches based on exact cancellations: the presumption of a perfect model; known parameters; and

noise-free high bandwidth state information. It is not clear how effectively this exact embedding can be implemented in a physical platform in the face of the inevitable actuator, computational, and sensory limitations.

2.2.2. *Passive Control*

An alternative to active control relies on the passive dynamics of the system combined with low-bandwidth controllers to anchor the SLIP template. Demonstrating that this may be possible represents the chief concern of the paper as established in §3. Even with a very simple open-loop control strategy, our study reveals the presence of certain “sweet spots” in the RHex parameter space, wherein the SLIP emerges naturally. It is still unclear whether this respects the formal “anchored template” paradigm wherein the lower dimensional dynamics actually appears as an attracting invariant dynamical submanifold. However, experimental evidence revealing the template behavior in steady state from various different initial conditions suggests there are, indeed, operating regimes where the system trajectories are attracted to the low dimensional SLIP template dynamics. Further evidence for the SLIP template comes from numerical studies using SimSect — a simulation package developed by Saranli [15]. SimSect was devised to approximate the behavior of RHex by numerically integrating a set of simplified equations of motion which are expected to govern RHex’s hybrid mechanical system. Currently, the same low-level controller as in RHex is implemented in SimSect. This makes SimSect an ideal test-bed for new control designs for RHex. Although an exact correspondence between RHex’s and SimSect’s parameter space has not yet been established, the simulation results in §3.4 lend credence to SimSect being a representative numerical approximation to RHex’s dynamics.

3. Finding the SLIP in RHex’s Motion

The central observations about cockroach locomotion that inform the design of the RHex prototype include: (i) that it operates via compliant legs; (ii) that its limb motions appear to be characterized by a strongly stereotypical “clock”; (iii) that it has a sprawled posture to enhance stability; and (iv) that the stabilizing controller must somehow be embedded in the very morphology itself. The impact of these observations for RHex are, indeed, directly apparent in the morphology and control approach that we have already reported. However, it is not obvious that we will find a SLIP in such a machine.

3.1. Data Collection, Experimental Setup and Procedures

In order to determine whether RHex passively anchors a SLIP, the ground reaction forces produced by RHex during locomotion were measured during 92 trials using two six-component force plates¹. The force and torque signals were amplified² and each channel was recorded at 1000Hz by an analog to digital converter³. Each trial was also recorded by a high speed video camera⁴.

¹Biomechanics Force Platform, Advanced Mechanical Technology, Inc., Newton, MA.

²Model SGA, Advanced Mechanical Technology, Inc., Newton, MA.

³PCI board, National Instruments, Austin, TX.

⁴MotionScope PCI 1000, Redlake Imaging, Morgan Hill, CA.

In our experiments, the robot started walking approximately two meters away from the force plates in order to allow the robot to settle into an approximate steady state motion upon encountering the plates. While the robot was in contact with the force plates no directional adjustment was made since this would otherwise have broken the open loop symmetry between the right and left leg motion profiles.

During the trials, four parameters were varied: leg type; ground material; robot mass; and forward speed. For a fixed set of parameters, the experiments were repeated between 4 and 8 times. The experiments started off with the slowest forward speed on the bare force plates with Delrin legs (stiffness $\kappa \approx 4300N/m$). Then the speed was increased in three steps by choosing different cycle times⁵ ($t_c \in \{1.2s, 0.8s, 0.53s, 0.5s\}$) without changing the physical structure. To reduce bounce and slippage, which was observed especially at high speeds, the surface of the force plates was then covered with an elastic foam mat, and the same speed sweep with the Delrin legs was performed. In the second round of the experiments, a new 4-bar linkage composite leg design ($\kappa \approx 3100N/m$) was used in conjunction with a similar speed sweep on both the bare force plates and the plates covered with the foam mat. Our preliminary observations during the first two trial runs suggested that the COM of the body behaves more like an inverted pendulum (IP) rather than a spring loaded inverted pendulum (SLIP). We reasoned that the leg-body system, which defines an overall lumped spring-mass system, has a much higher natural frequency than the stride frequency achievable by the hip actuators. In order to test this hypothesis, in the third round of the experiments, the body mass was increased, effectively decreasing the natural frequency of the spring-mass system. We ran the robot with composite legs at the highest speed setting on the elastic mat. Its mass was increased incrementally from $7.83kg$ to $9.47kg$ to $11.12kg$ to $11.94kg$. In the highest mass regime we observed the transition from IP to SLIP reported below.

3.2. Data Extraction

The data plotted in Fig. 1 arise from the summed leg or COM ground reaction forces imparted to the legs by the ground plate while the robot performs an alternating tripod gait. To remove noise from the recorded data, the forces were filtered using a second order Butterworth filter with a cutoff frequency of 50Hz. The minima of the vertical force data were used to isolate single strides. Since a stride is a complete cycle for all the legs, it contains two steps for each tripod and therefore two minima. Only strides from the middle section of the data for one force platform — where the force data exhibited oscillatory behavior of one predominant frequency and roughly constant amplitude — were selected. Only those trials where the maximum of the power spectrum $P(f)$ occurs at twice the cycle frequency⁶ $f_c = 1/T_c$ were used, in rough accord with the

⁵The motion profile utilized by RHex is parametrized by cycle time, sweep angle, leg offset and flight time (for a detailed description of these parameters see [15]). For each forward speed setting a different set of values is assigned to these four parameters.

⁶During one cycle, two steps are taken.

criterion established in [16] to distinguish walking from running.⁷ These criteria reduced the number of available trials to be used for SLIP fitting from 92 to 14. Since the force platform is very narrow with respect to the width of RHex and only those trials for which RHex stayed on the track were recorded, the lateral force data are not used in this investigation.⁸ This restriction respects the intended limitations on our scope of analysis in this initial study to the saggital plane only.

Unfortunately, the camera’s resolution was not good enough to provide integration constants for vertical and fore/aft speeds and positions at the beginning of each stride, required for our fitting study. Instead, the initial vertical speed is indirectly obtained from the assumption of periodicity – namely, that after one stride, the robot returns to its initial height. Similarly, the fore/aft initial speed is calculated by matching the average velocity over one stride to the average velocity over both force plates. The initial height is assumed to be at RHex’s static equilibrium with all legs vertical to the ground (0.164m).

3.3. Data Analysis

The SLIP template imposes a very particular set of relationships — those specified by the Lagrangian mechanics of a single point mass prismatic-revolute (i.e., polar coordinate) kinematic chain between the ground reaction forces, motion of the COM, and system energies. Ruina has pointed out [19] that any convex curve supports in a neighborhood of its vertical minimum at least one time varying trajectory generated by some SLIP. RHex’s COM inevitably rides along a convex curve: we wish to understand whether its actual time trajectory along this curve can be readily generated by some SLIP model.

3.3.1. A Protocol for Fitting SLIP to RHex’s Running Data

The 14 remaining trials that satisfy the criteria in §3.2 are now used to test the presence of the SLIP template in RHex according to an adaptation of the methodology introduced in [11]. For each of the 136 steps (68 strides) in the 14 trials, a SLIP model is fit using ordinary least squares regression. Fitting a SLIP model to these data is not entirely straightforward: since RHex did not

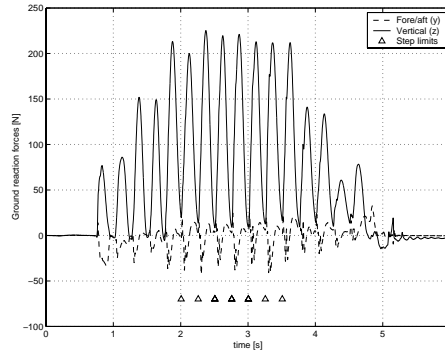


Figure 1. Ground reaction forces for trial 6 (comp. legs, foam mat, $t_c = 0.5s$, $m = 11.94kg$). The triangles denote the beginning and the end points of steps selected for fitting.

⁷Specifically, the ratio of the integrated power spectrum around the maximum to the total integrated power spectrum was required to satisfy $(\int_{2f_c-\epsilon}^{2f_c+\epsilon} P(f)df)/(\int_0^\infty P(f)df) > 0.8$, where ϵ was appropriately chosen to include the global maximum alone.

⁸The magnitude of the lateral forces is comparable to the one for the fore/aft forces. A complete template should incorporate lateral forces, see e. g. [17] or [18].

exhibit any flight phase, the touchdown and lift-off points are not defined. In contrast, if the anchoring hypothesis has any validity, then the region around a bottom should be well described by a SLIP stance phase. Absent a specific model for determining the limits of this region, we adopt the ad hoc condition determined by the point of zero crossing of the vertical COM force.⁹

Fitting data to this central force model requires knowledge of the center of pressure (the pivot point of the virtual SLIP), which could not be determined with our experimental equipment. As a reasonable work-around, we assume that the center of pressure lies directly below the vertical minimum. This in turn, implies that the SLIP model operates at equilibrium on a “neutral orbit” [3, 11] characterized by this symmetry. However, the measured force data are not perfectly periodic, hence the integrations to yield velocity and position are necessarily not periodic, either. Notwithstanding this slight conceptual conflict, we see no better method for selecting the nominal center. These assumptions in force, the data population for SLIP fitting can be restricted to range only from a vertical minimum to the next zero crossing of the vertical force.

Given a COM trajectory fragment, $\{\mathbf{b}(\mathbf{t}), \dot{\mathbf{b}}(\mathbf{t}), \ddot{\mathbf{b}}(\mathbf{t})\}_{t_0=T_{bottom}}^{t_N=T_{liftoff}}$, the COM position¹⁰ $\mathbf{b} = (y \ z)^\top$ and acceleration $\ddot{\mathbf{b}}$ are fitted to a Hooke spring law with unknown spring length¹¹ q_{r0} and spring stiffness κ :

$$\frac{\mathbf{b}}{\|\mathbf{b}\|}(\kappa_1 - \kappa_2\|\mathbf{b}\|) = m(\ddot{\mathbf{b}} - \mathbf{g}) ,$$

where $\kappa = \kappa_2$ and $q_{r0} = \frac{\kappa_1}{\kappa_2}$. Note that this model is linear in parameters so that ordinary least squares applies directly.

The assessment of the quality of the fit proceeds in two steps. First, a SLIP simulation over the same period of time as the data trajectory is run with the values of κ and q_{r0} obtained in the first step. The initial conditions are taken to be the positions and velocities of the data trajectory at the minimum. Second, the resulting SLIP trajectories $z^{\text{SLIP}}, \dot{z}^{\text{SLIP}}, y^{\text{SLIP}}, \dot{y}^{\text{SLIP}}$ are compared to the data trajectories by L_1 and L_2 percent errors:

$$\Delta X_{L_1} = 100 \frac{\|X - X^{\text{SLIP}}\|_1}{\text{Range}(X)} , \quad \Delta X_{L_2} = 100 \frac{\|X - X^{\text{SLIP}}\|_2}{\|X\|_2} ,$$

where $\text{Range}(X) = |\max(X) - \min(X)|$. Here, $\|X\|_p = (\int_{t_0}^{t_1} |X(t)|^p dt)^{\frac{1}{p}}$ and $X \in \{z, y, \dot{z}, \dot{y}\}$.

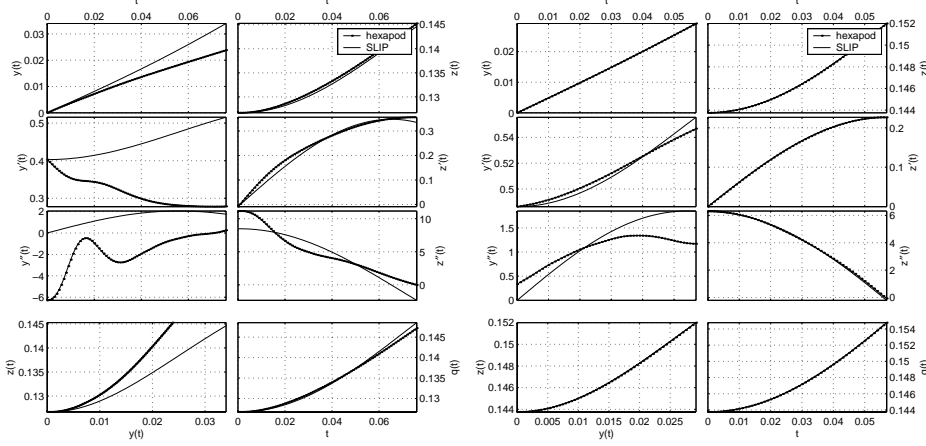
In an effort to simplify the assessment of the fitting error, the quality of the fit is reported as a single number — the average L_p percent error $\Delta_{L_p} = (\Delta z_{L_p} + \Delta y_{L_p} + \Delta \dot{z}_{L_p} + \Delta \dot{y}_{L_p})/4$.

⁹Presumably, the phase interval corresponding to flight in the simple SLIP template must be replaced with an appropriately more complex (but still low dimensional) model. Since we have not yet developed this model, we rely on the ad hoc termination criterion.

¹⁰In this notation, z gives the co-ordinates in the vertical direction and y gives the co-ordinates in the fore/aft direction relative to an inertial frame located at the center of pressure.

¹¹Fitting the spring length q_{r0} alleviates the arbitrariness of selecting the equivalent lift-off point for RHex data, because now the zero crossing of the vertical COM force need not correspond to the lift-off point of the fitted SLIP model.

As an illustration of the fitting results, the worst and the best SLIP fits amongst the 136 steps are presented in the next figure. The data trajectories



(a) RHex trial no. 2, 4th stride, 2nd minimum (composite legs, foam mat, $t_c = 0.5s$, $m = 11.12kg$) incurs the largest SLIP fitting error of $\Delta_{L_2} = 21.6\%$.

(b) RHex trial no. 10, 5th stride, 1st minimum (composite legs, foam mat, $t_c = 0.5s$, $m = 11.94kg$) incurs the smallest SLIP fitting error of $\Delta_{L_2} = 0.3\%$.

Figure 2. Worst and best SLIP fits: Dotted lines represent experimental data; solid lines represent SLIP trajectories with fitted values κ and q_{r0} .

of $y(t)$, $\dot{y}(t)$, $\ddot{y}(t)$, $z(y)$, $z(t)$, $\dot{z}(t)$, $\ddot{z}(t)$, and $q(t) = \sqrt{y^2(t) + z^2(t)}$ (dotted lines) are plotted together with the SLIP predictions computed with the fitted stiffness κ and spring length q_{r0} . The worst SLIP fit with $\Delta_{L_2} = 21.6\%$ is shown in Fig. 2(a), in contrast to $\Delta_{L_2} = 0.3\%$ in Fig. 2(b).

As an internal consistency check, we introduce a simple form of cross validation: The available COM trajectory components $X \in \{z, y, \dot{z}, \dot{y}\}$ each comprising a time sampled fragment of length N are partitioned by $r = \lfloor N/20 \rfloor$, sub-sampling them into a fitting population X_{fit}^i , $i \in \{1, \dots, r\}$ of length $N_{fit} = \lfloor N/r \rfloor$ and its complement $X_{cross}^i = X \setminus X_{fit}^i$ — the cross validation populations. The fitting procedure is applied to a fitting population X_{fit}^i to yield κ^i and q_{r0}^i . The quality of fit is assessed not only on X_{fit}^i but also on the corresponding cross-validation population X_{cross}^i with κ^i and q_{r0}^i obtained from X_{fit}^i . In Table 1 the fitting errors $\Delta_{L_p, fit}^i$ and cross validation errors $\Delta_{L_p, cross}^i$ are subsumed under $\Delta_{L_p, fit} = \text{mean}\{\Delta_{L_p, fit}^i\}_{i=1}^r$ and $\Delta_{L_p, cross} = \text{mean}\{\Delta_{L_p, cross}^i\}_{i=1}^r$, and the standard deviations $\text{std}\{\Delta_{L_p, fit}^i\}_{i=1}^r$ and $\text{std}\{\Delta_{L_p, cross}^i\}_{i=1}^r$.

In addition to the L_1 and L_2 errors that compare the experimental data to fitted SLIP predictions, experimental measurement errors introduce noise into the data. To evaluate the quality of fit, one must compare the relative noise

floor, $\delta X/\text{Range}(X)$ to the L_1 fitting errors. The noise floor comes from two sources: the measurement error of the ground reaction forces, and the uncertainties of the integration constants for the velocity and position trajectories. In Table 1 the estimated relative noise floors for the z, y, \dot{z}, \dot{y} trajectories are averaged over each stride.

3.3.2. Evidence for SLIP in RHex Running

The fitting protocol outlined in the previous section is now applied to all 136 steps¹². For the sake of brevity, we refrain from listing the fitted parameters and the fitting errors for each step. Instead, average values over all steps are calculated together with the standard deviation. The mean fitted stiffness is $\kappa = (6100 \pm 940)N/m$, and the mean fitted relaxed spring length is $q_{r0} = (0.171 \pm 0.007)m$. The results of the error analysis are listed in Table 1.

(%)	ΔL_p	$\Delta L_{p,fit}/\Delta L_{p,cross}$	$\Delta L_{p,cross}$	$\text{std}(\Delta L_{p,cross})$
L_2	0.069 ± 0.054	0.985 ± 0.013	0.069 ± 0.054	0.001 ± 0.001
L_1	0.258 ± 0.197	1.002 ± 0.012	0.259 ± 0.199	0.004 ± 0.006
(%)	Δy_{L_1}	Δz_{L_1}	$\Delta \dot{y}_{L_1}$	$\Delta \dot{z}_{L_1}$
L_1	0.041 ± 0.036	0.010 ± 0.010	0.96 ± 0.78	0.020 ± 0.018
Noise floor	0.009	0.003	0.38	0.009

Table 1. Error analysis of SLIP fitting to 136 steps.

The average ΔL_2 error of $\approx 7\%$ seems to be remarkable for a mechanical device that a priori bears to resemblance to a SLIP model. The L_1 average percent errors are all similarly low, except for the \dot{y} fits, which are corrupted in part by the high noise floor (see discussion at the end of §3.3.1) and in part by real discrepancies with the putative model, for example, as depicted in Fig. 2. Since the component-wise L_1 errors are considerably above the noise floor, and since the L_p fitting and cross validation errors are comparable, there is little concern that we are merely fitting to noise.

The question naturally arises why we only present fitting results for the decompression phase interval of the COM data instead of the whole compression-decompression phase interval between the zero-crossings of the vertical force. After all, this alternative would serve as a test of our neutral orbit assumption (see §3.3.1). Indeed, the fitting errors for the compression phase interval are of comparable magnitude to the ones for decompression above. However, the fitted spring stiffness is higher and its standard deviation over all 136 steps is twice as large as compared to the decompression phase interval study reported here. An explanation might be the more frequent occurrence of “double stance” (more than 3 legs on the ground) during compression than decompression. This is in fact observed in sample SimSect simulations. As double stance events alter the dynamics of the robot, we single out the decompression phase interval of the COM data as the likeliest candidate of the trajectories for the

¹²In all the selected experiments, RHex operated in the highest speed setting with the composite leg design and the elastic foam ground. Moreover, they were mainly experiments with high body masses: 8 runs with $m = 11.94kg$, 5 runs with $m = 11.12kg$ and 1 run with $m = 9.47kg$.

validation of the SLIP model.

3.4. Supporting Numerical Study

3.4.1. SLIP Fitting in SimSect

The previous sections suggest that the SLIP model provides a good low dimensional approximation to the “stance” dynamics of RHex. In this section, we describe a parallel numerical investigation of SimSect simulations to determine the “sweet spots” wherein the hexapod might actually be presumed to anchor the SLIP. Specifically, we show that SLIP-like behavior of the mechanical system modeled by SimSect occurs in specific ranges of SimSect’s parameter space.

In order to compare the SLIP fitting results from SimSect to those from RHex experiments, the same decompression phase interval as in §3.3.1 is used for fitting.¹³ Only those runs where exactly 3 legs of the same tripod are on the ground at the vertical minimum were considered to be acceptable; this was inspired by the assumption that the jointly controlled three legs, which constitute a tripod, can be thought of as a virtual SLIP leg and reflects our experimental experience. As an additional filter, only those simulations which exhibit periodic behavior after a certain amount of time are used for fitting to the SLIP model.

The simulations are run for a fixed set of physical parameters (e.g. total mass, moments of inertia, etc.) and initial conditions, whereas the control parameters sweep angle, cycle time, and leg offset¹⁴ are varied in certain ranges described below. The flight time is chosen to be ≈ 0.4 the cycle time in order to match the highest speed setting for RHex. With force, velocity, and position data from SimSect simulations, the fitting procedure is carried out as in §3.3.1.

3.4.2. Fitting Results

Although SimSect is modeled with many simplifications respecting the actual robot, RHex’s main dynamical features are believed to be incorporated in SimSect. Hence the SimSect simulations were run in parameter regimes that include the high mass, high speed regimes of RHex where good SLIP fits could be obtained. In particular, with total mass $m = 11.9kg$, sweep angle = $0.44 \dots 0.76rad$, cycle time = $0.42 \dots 0.54s$, leg offset = $0 \dots -0.15rad$, and individual leg stiffnesses $\kappa \approx 2700N/m$, SLIP like behavior could be found in SimSect, too. This is demonstrated in Fig. 3, which shows — on the left side — a histogram of the number of simulations from the above listed parameter range with respect to the average L_2 error, Δ_{L_2} . The total number of simulations is reported above the histogram. For comparison, a two-parameter exponential distribution is fit to the histogram bins. On the right side a graph shows the average L_2 error Δ_{L_2} as a function of two of the four control parameters: cycle time and sweep angle. The flight time is kept proportional to the cycle time and only a small dependence of Δ_{L_2} on the leg offset was observed.

¹³In SimSect, information about which legs are on the ground and which are not is, of course, available. A detailed investigation of the quality of the SLIP fitting as a function of footfall patterns will be the subject of a future report.

¹⁴For a detailed description of SimSect’s parameter space, see [15].

Instead of a scatter plot, a quadratic surface is fit to the data, and the spread of the data is characterized by its second moment around the surface, which is represented by vertical bars at the corners of the surface. For all SimSect

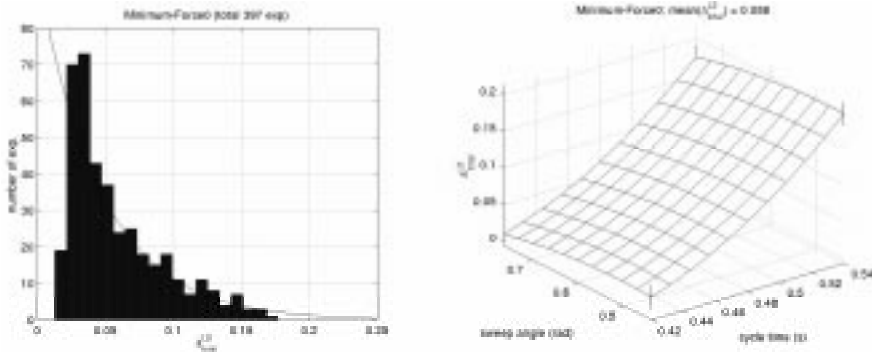


Figure 3. Average errors Δ_{L_2} for SimSect SLIP fits. The left side shows a histogram of the number of simulations; the right side shows a map of Δ_{L_2} as a function of the (reduced) control parameter space.

simulations the ratio of the average fitting to the average cross validation error $\Delta_{L_2,fit}/\Delta_{L_2,cross}$ did not deviate by more than 10% from unity, thus providing a successful self-consistency check for our fitting procedure. The results in this section, in particular the low average fitting errors of $\approx 6\%$ in Fig. 3 lend strong support to the presumption that the SLIP template may be anchored in SimSect’s dynamics.

4. Conclusion: Implications for More Autonomous Control of RHex

Hierarchy promotes the use of few parameters to control complex systems with many degrees of freedom. In this light, as we understand matters, the emergence of an anchored SLIP in RHex is most fortunate. The pogo-stick can function as a useful control guide in developing more complex autonomous locomotion behaviors such as registration via visual servoing, local exploration via visual odometry, obstacle avoidance, and, eventually, global mapping and localization. In the longer term, we propose to work with the anchored SLIP in RHex in analogy to the manner in which the simple two-bead template has been exploited in juggling. Namely, as we shape behavior via manipulation of gains-in-the-loop [20], we hope to develop a formal programming language with semantics in the world of dynamical attractors [21].

Acknowledgements

This work is supported by DARPA/SPAWAR under contract N66001-00-C-8026. We thank Rodger Kram and Claire Farley for the use of the force platform, Irv Scher for collaboration at an early stage of this project and William Schwind for the insight and the analytical tools he provided.

References

- [1] Saranli U, Buehler M and Koditschek D E 2000 Design, Modeling and Preliminary Control of a Compliant Hexapod Robot. *Proc. IEEE Int. Conf. Rob. Aut.* 3:2589-2596.
- [2] Blickhan R and Full R 1993 Similarity in multilegged locomotion: Bouncing like a monopode. *J. J. Comp. Physiol. A* 173, 509-517.
- [3] Raibert M 1986 *Dynamic Robots that Balance*, MIT Press, Cambridge.
- [4] Schwind W J and Koditschek D E 2000 Approximating the Stance Map of a 2 DOF Monoped Runner. *Journal of Nonlinear Science* 10:533-568.
- [5] Saranli U, Schwind W J, and Koditschek D E May 1998 Toward the Control of Multi-Jointed, Monoped Runner. *IEEE Int. Conf. on Rob. and Aut.* Leuven, Belgium pp 2676-2682.
- [6] Full R J and Koditschek D E 1999 Templates and Anchors: Neuromechanical Hypotheses of Legged Locomotion on Land. *J. Exp. Bio.* 202:3325-3332.
- [7] Koditschek D E and Bühler M Dec 1991 Analysis of a simplified hopping robot. *International Journal of Robotics Research* 10(6):587-605.
- [8] Bühler M, Koditschek D E, and Kindlmann P J 1990 A Family of Robot Control Strategies for Intermittent Dynamical Environments. *IEEE Control Systems Magazine* 10(2):16-22.
- [9] Rizzi A A, Whitcomb L L, and Koditschek D E 1992 Distributed Real-Time Control of a Spatial Robot Juggler. *IEEE Computer* 25(5):12-24.
- [10] Nakanishi J, Fukuda T, and Koditschek D E 2000 A Brachiating Robot Controller. *IEEE Trans. Rob. Aut.* 16(2):109-123.
- [11] Schwind W J 1998 Spring Loaded Inverted Pendulum Running: A Plant Model. PhD thesis, University of Michigan.
- [12] Full R J and Farley C T 2000 Musculoskeletal Dynamics in Rhythmic Systems: A Comparative Approach to Legged Locomotion. In: Winter, Crago (eds) *Biomechanics & Neural Control of Posture & Movement* Springer Verlag, New York, pp 192-205.
- [13] Hogan N Mar 1985 Impedance Control: An Approach to Manipulation. *ASME Journal of Dynamic Systems, Measurement, and Control* 107:1-7.
- [14] Pratt J and Pratt G May 1998 Intuitive Control of a Planar Bipedal Walking Robot *ICRA* Leuven, Belgium pp 2014-2021.
- [15] Saranli U 2000 SimSect Hybrid Dynamical Simulation Environment. *University of Michigan Technical Report* CSE-TR-437-00.
- [16] Alexander R McN 1992 A Model of Bipedal Locomotion on Compliant Legs *Phil. Trans.: Biol. Sc.* 338(1284):189-198.
- [17] Carver S 2000 The Limits of Deadbeat Control for the Spatial SLIP. in preparation.
- [18] Schmitt J and Holmes P 2000 Mechanical models for insect locomotion: Dynamics and stability in the horizontal plane I: Theory; II: Application. *Biological Cybernetics* 83(6):501-515 and 517-527.
- [19] Ruina A, personal communication.
- [20] Burridge R R, Rizzi A A, and Koditschek D E 1999 Sequential Composition of Dynamically Dexterous Robot Behaviors. *Int. J. Rob. Res.* 18(6):534 - 555.
- [21] Klavins E and Koditschek D E 2000 A formalism for the composition of concurrent robot behaviors. *Proc. IEEE Conf. Rob. and Aut.* 4:3395 - 3402.